Model of Oligomer Formation

The premise for the model below is that each peptide monomer can adopt a variety of conformations through intramolecular diffusion. These conformations can be divided into two states, those that have hydrophobic patches exposed to solvent (M^*) and those that don't (M). Only those that have hydrophobic patches exposed to solvent can make stable dimers. A full model of all dimers that can be formed is

$$
\begin{array}{l}
M \underset{k_{-1}}{\overset{k_1}{\rightleftarrows}} M^* \\
M^* + M^* \underset{k_d}{\overset{k_+^{bi}}{\rightleftarrows}} [M^* M^*] \underset{k_{-O}}{\overset{k_O}{\rightleftarrows}} O \\
\qquad\qquad k_1 \updownarrow k_{-1} \\
M + M^* \underset{k_-^{bi}}{\overset{k_+^{bi}}{\rightleftarrows}} [MM^*] \\
\qquad\qquad k_1 \updownarrow k_{-1} \\
M + M \underset{k_-^{bi}}{\overset{k_+^{bi}}{\rightleftarrows}} [MM]
\end{array}
\qquad \text{(i)}
$$

We make several assumptions:

1) The formation of O is irreversible; that is, $k_{-O} \sim 0$
2) $k_O << k_+^{bi}$.
3) It is not possible to measure the reconfiguration of encounter complexes, since they are extremely unstable. We assume that their reconfiguration is the same as for the monomers, as they comprise of loosely bound monomers.
4) Since there are no stabilizing interactions for $[MM]$ and $[MM^*]$, the dissociation rate for these complexes is purely diffusive, k_-^{bi} is much faster than all other rates in the scheme.
5) Bimolecular dissociation constants depend on the stabilizing interactions of the encounter complex. k_d is much smaller than k_-^{bi} because there are attractive hydrophobic interactions in $[M^*M^*]$.

To avoid going irreversibly to O, $[M^*M^*]$ can dissociate to M^* and M^* or reconfigure to $[MM^*]$. Thus, for $k_{-1} >> k_d$, the primary flux of dissociation is through [MM*]. This complex is not very stable and so the complex immediately comes apart. Therefore, for k_{-O} and k_d sufficiently slow, and k_-^{bi} sufficiently fast, the model can be approximated by scheme (ii), which has been used in previous versions of this model

$$M \underset{k_{-1}}{\overset{k_1}{\rightleftharpoons}} M^*$$

$$M^* + M^* \xrightarrow{k_{bi}} [M^* M^*] \xrightarrow{k_O} O \qquad \text{(ii)}$$

$$\downarrow k_{-1}$$

$$M + M^*$$

Mutant	Temperature (C)	σ	<*r*> (Å)
wildtype	20	1.2	32.9
A53T	20	1.6	31.7
E46K	20	> 2.5	< 29.5
A30P	20	1.0	33.5
V74E	20	1.5	32.0
T72P	20	1.6	31.7
wildtype	30	> 2.5	<29.5
A53T	30	> 2.5	< 29.5
E46K	30	> 2.5	< 29.5
A30P	30	> 2.5	< 29.5
V74E	30	1.5	32.0
T72P	30	1.6	31.7

Table S1. Energy re-weighted WLC model of experimental measurements. Tuning parameter, σ, are the best fits to the measured k_R for a particular temperature and mutant. The average distance, $< r >= \int rZ(r)dr$ for each distribution is also shown.

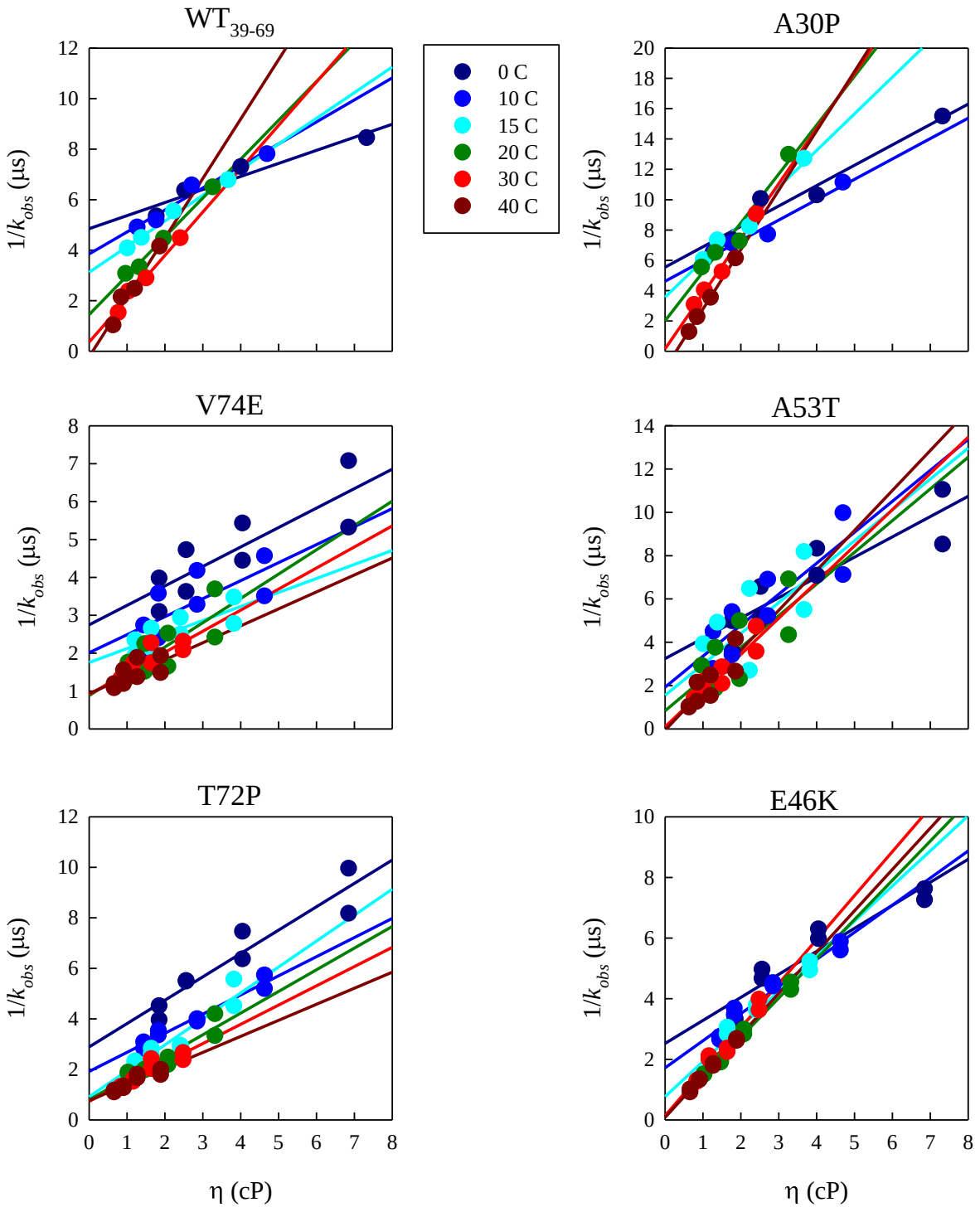

Figure S1. Measured Trp triplet decay times vs. solution viscosity for different mutants as marked. The colors represent different temperatures as marked and lines are linear fits to the data at a single temperature.

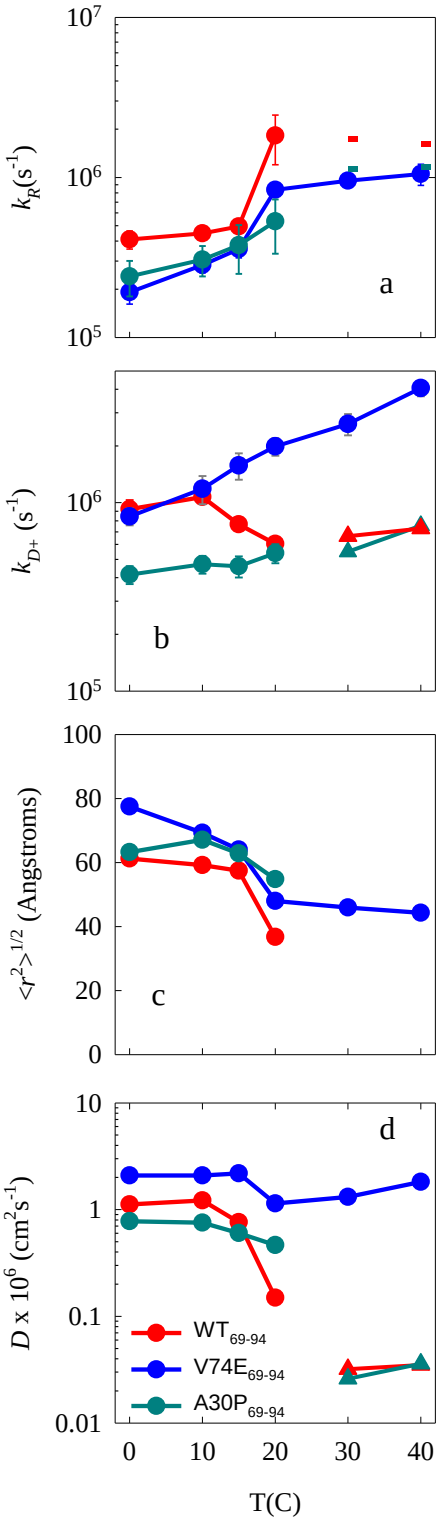

Figure S2. a) Reaction-limited rates of WT_{69-94}, A30P and V74E placed in the 69-94 loop. The rate at 30 and 40 C for the wildtype and A30P are too fast to be quantitatively determined and the dashes represents the lower limit. b) Diffusion-limited rates, normalized to the viscosity of water at that temperature. At T=30 and 40 C the observed rates are diffusion limited ($k_{obs} \sim k_{D+}$) and are plotted as triangles. c) Average root mean square distance between the Trp and Cys

determined for each reaction-limited rate using Eq. 4 and Eq. 6. d) Intramolecular diffusion coefficients determined for each diffusion-limited rate using Eq. 5. (triangles) D determined from values in (b) using Eq. 3 and $\langle r^2 \rangle = 400 \pm 100$ Å^2. The error bars are the propagated error of k_{D+} and $\langle r^2 \rangle$.